

Different methods in TiO₂ photodegradation mechanism studies: Gaseous and TiO₂-adsorbed phases

Pierre-Alexandre Deveau^a, Fabrice Arzac^b, Pierre-Xavier Thivel^{a,*}, Corinne Ferronato^b,
Françoise Delpech^a, Jean-Marc Chovelon^b, Pascal Kaluzny^c, Christine Monnet^d

^a *Groupe de Recherche sur l'Environnement et la Chimie Atmosphérique, Université Joseph Fourier Grenoble I, France*

^b *Laboratoire d'Application de la Chimie à l'Environnement, Université Claude Bernard Lyon I, France*

^c *Tera Environnement, Grenoble, France*

^d *Ahlstrom Research and Services, Pont Evêque, France*

Available online 30 January 2007

Abstract

The development of photocatalysis processes offers a significant number of perspectives especially in gaseous phase depollution. It is proved that the photo-oxidizing properties of photocatalyst (TiO₂) activated by UV plays an important role in the degradation of volatile organic compounds (VOC). Heterogeneous photocatalysis is based on the absorption of UV radiations by TiO₂. This phenomenon leads to the degradation and the oxidation of the compounds, according to a mechanism that associates the pollutant's adsorption on the photocatalyst and radical degradation reactions.

The main objective of the study is the understanding of the TiO₂-photocatalysis phenomenon including gaseous and adsorbed phase mechanisms.

Results obtained with three different apparatus are compared; gaseous phases are analysed and mechanisms at the gaseous phase/photocatalyst interface are identified.

This study leads to improve understanding of various mechanisms during pollutant photodegradation: adsorption of pollutants on TiO₂ first takes place, then desorption and/or photodegradation, and finally, desorption of degradation products on TiO₂. The association of analytical methods and different processes makes the determination of all parameters that affect the photocatalytic process possible. Mastering these parameters is fundamental for the design and construction of industrial size reactors that aim to purify the atmosphere.

© 2007 Elsevier B.V. All rights reserved.

Keywords: Photocatalysis; TiO₂; Toluene; Gas phase; Gas–solid interface; Photoreactors; Trace level; FT-IR spectroscopy; Gas chromatography

1. Introduction

The development of photocatalysis processes offers a significant number of perspectives, especially in gaseous phase depollution. It is proved that the photo-oxidizing properties of the TiO₂ semi-conductor activated by UV radiations play a major role in the degradation of the volatile organic compounds (VOC), both malodorous and pollutant.

Photocatalysis processes are based on the absorption of UV radiation by the photocatalyst (titanium dioxide). This phenomenon leads to the oxidation and the degradation of the compounds according to numerous mechanisms that associate the pollutant's adsorption [1] on the photocatalyst and radical

degradation reactions [2,3] where OH• radicals are the first reagents. The final result can be, in optimal conditions, the complete mineralisation of all pollutants into CO₂ and H₂O and possibly inorganic salts.

However, the development of these complex mechanisms can vary depending on the running conditions of the experiments: diverse photoreactor designs exist and are on the market.

The aim of this study is to compare photocatalysis yield with three different systems and to understand the TiO₂-photocatalysis phenomenon including gaseous and adsorbed phase mechanisms.

To lead this research program, we use three reactors whose main running characteristics are set out below:

- The first one (P1), specially designed for this research project, leads to the study of adsorption and degradation mechanisms at the gaseous phase/photocatalyst interface.

* Corresponding author at: 39-41 Boulevard Gambetta, 38000 Grenoble, France.

E-mail address: Pierre-Xavier.Thivel@ujf-grenoble.fr (P.-X. Thivel).

- The second one (P2) is a continuous mixed flow reactor, where the VOC has both a licking and a crossing trajectory through the TiO₂-photocatalytic filter.
- The third one (P3) is also a continuous photoreactor where the pollutants have a crossing trajectory through the TiO₂ filter.

It is important to note that both systems P2 and P3 work with dynamic running conditions with complementary scale of VOC concentrations in gaseous phase: P2 is designed to reach high concentration ($1\text{--}15 \times 10^{-3} \text{ g m}^{-3}$) and P3 is well adapted for concentrations less than $1 \times 10^{-3} \text{ g m}^{-3}$.

In this paper, we present the degradation of toluene using these three laboratory plants. The following sub-topics are developed: the description of the experimental plants (photoreactor and analytical methods), then comparison and discussion of results with the determination of conversion rates and kinetics constants.

2. Experimental methods

2.1. Materials

The photocatalyst used is TiO₂ PC500 provided by Mille-nium. It is 100% anatase, is characterized as having an average particle size of about 10 nm and a specific area of around $350 \text{ m}^2 \text{ g}^{-1}$.

For the P1 photoreactor, the PC500 TiO₂ catalyst is used without further purification. The TiO₂ powder is pressed into self-supporting pellets (about $200\text{--}300 \text{ g m}^{-2}$), and then placed in an IR Pyrex cell, equipped with CaF₂ windows.

For the continuous flow reactors, the catalyst used is a fibrous substrate coated with PC500 TiO₂ (15 g m^{-2}) and using an inorganic binder. This catalyst is sold by Ahlstrom Company (Pont-Eveque, France).

2.2. Photoreactors

The P1 photoreactor [5], the FT-IR in situ experiment, provided information about the gas–solid interface during the photocatalytic degradation experiment. This laboratory plant allowed the formation and disappearance of the species adsorbed during the degradation to be identified and followed.

Fig. 1 shows a diagram of the FT-IR experimental set-up. This apparatus consists of three main parts.

The first one allows the introduction of the reactants (VOC, H₂O, N₂, O₂). This part of the reactor is connected to a vacuum pump. Gaseous VOC and water vapor introduced are monitored by measuring their partial pressure in the reactor.

The middle section of the reactor is the quartz tube fitted out with a furnace, allowing thermal treatment at high temperature (up to 500 °C).

The bottom part of the reactor is made of Pyrex IR cell, cooled at room temperature by water circulation.

In the photo-oxidation experiments, the pellet is irradiated through the Pyrex walls of the IR cell; the irradiation source is an UV HPK 125 W lamp from Philips. A water cell is placed in front of the UV lamp to prevent TiO₂ heating during irradiation.

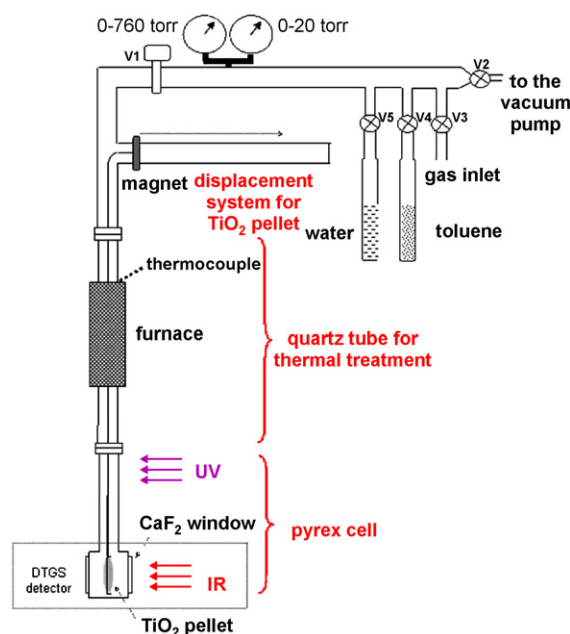


Fig. 1. Photoreactor P1.

In these conditions, the irradiation energy at the position of the TiO₂ sample is 32 mW cm^{-2} . An appropriate magnetic system is used to move the sample holder containing the TiO₂ pellet up and down, in front of the irradiation lamp and in the IR beam for surface analysis.

The characteristics of the P2 photoreactor [4] are as follows: cylindrical geometry, 4 cm inner diameter, whose accessible volume to the VOC is 0.210 L, equipped with an external irradiation and a double wall to ensure the permanent cooling of the photodegradation cell with fresh water. The inflow is 1 L/min with varying toluene concentrations from 1 to $15 \times 10^{-3} \text{ g m}^{-3}$. The TiO₂ support also has a cylindrical shape (Fig. 2).

The photoreactor is included in a laboratory pilot plant with a 200 L gaseous effluent preparation reactor, a dilution inflow circuit, a humidification cell, various measurements (mass flow controller, temperature and relative humidity sensor, etc.), a sampling and testing cell into which the photoreactor gaseous

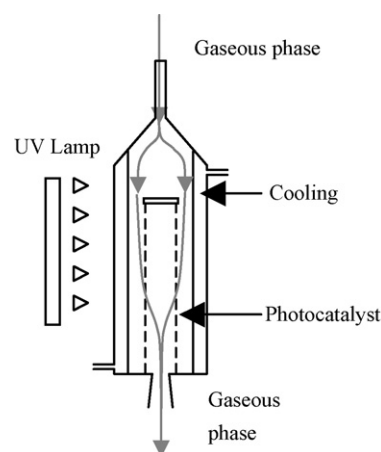


Fig. 2. P2 photoreactor.

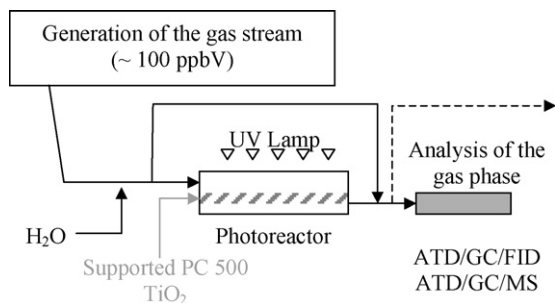


Fig. 3. P3 photoreactor.

outflow is fed. Finally, a pump controls the gaseous flow along the experimental set-up and prevents pressure drop.

The area of TiO₂-photocatalyst in the photoreactor is about $12 \times 10^{-4} \text{ m}^2$. The experiments are carried out using a Pyrex reactor and the irradiation system is the same as the one used with the P1 photoreactor. The UV radiations are filtered by the circulating water cell at average 365 nm wavelength. All connexions for gaseous flow circulation are done with Teflon tubing.

The third apparatus P3, shown in Fig. 3, is a continuous gas flow photoreactor. With this apparatus, we are able to obtain information about the gas phase during the photocatalytic degradation of volatile organic compounds at low concentration in the gas phase.

The VOC gaseous stream generation is carried out using a permeation system from Calibrage (France). Commercial permeation tubes are used. Brooks mass flow controllers 5850S series, in the 0–200 mL/min range, control the flow of the permeation oven and the dilution stream.

The humidifier system consists of a gas–liquid surface contactor with a liquid level and temperature control. The relative humidity of the dilution flow can be regulated in the range of 0–95%. Experiments are carried out at room temperature: $25 \pm 1 \text{ }^\circ\text{C}$. The gas stream humidity and temperature are measured using a thermohygrometer (Rotronic Hygropalm 1, France).

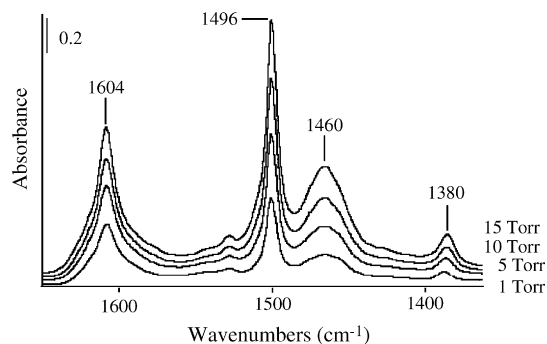
The photoreactor (volume of about $85 \times 10^{-6} \text{ m}^3$) is a cylindrical stainless steel reactor, containing the same supported PC500 TiO₂ as the one used with P2 photoreactor. In our configuration, the entering gas stream is passing through the supported TiO₂. The irradiation source is the same system as the one used with the P1 and P2 photoreactors. The light is passed through the top of the reactor, a Pyrex window. In this condition, the light intensity at the surface of the supported TiO₂ is 2 mW cm^{-2} . The irradiated surface is $1.20 \times 10^{-3} \text{ m}^2$.

In the case of the toluene study, the permeation rate is 117 ng min^{-1} at $50 \text{ }^\circ\text{C}$. The gaseous concentration of toluene can range from 4×10^{-5} to $3 \times 10^{-3} \text{ g m}^{-3}$. The flow rate in the reactor can vary from 0.05 to 0.5 L min^{-1} .

2.3. Analytical methods

The analytical methods depend on the photoreactor used.

P1: the IR spectra (4 cm^{-1} resolution) of TiO₂ self-supporting pellets were recorded with a Brücker IFS-28

Fig. 4. FT-IR spectra of adsorbed toluene on TiO₂.

spectrometer both in the absence and in the presence of adsorbed reacting species. Fig. 4 shows toluene adsorbed on TiO₂ for different toluene pressures in the reactor. These spectra are presented after subtraction of the TiO₂ spectrum. IR bands due to adsorbed toluene are observed at 1604, 1496, 1460 and 1380 cm^{-1} . Those IR bands were identified according to the literature. The 1604 and 1496 cm^{-1} peaks both correspond to the C=C aromatic ring vibrational [6–8] and the 1460 and 1380 cm^{-1} peaks both correspond to the CH₃ bending mode [6,8].

For photodegradation performed with P2 and P3, because of the trace concentrations of VOC in air, sampling of the gas phase is done using solid sorbent pre-concentration and further automatic thermodesorption coupled with gas chromatography equipped with flame ionisation detection for the quantification of VOC or mass spectrometry for the identification of the degradation products during the photocatalysis experiment.

For reactions performed with P2, sampling is carried out with a Smart Automated Sampling System (SASS) system designed by a cooperation between the GRECA laboratory and TERA Environnement company. The sampling times are from 1 to 5 min, with a 0.1 L/min flow and with a 6 min frequency.

The analytical instruments are from Perkin-Elmer (Turbomatrix ATD/Gold GC/MS for P2 and ATD Turbomatrix/Clarus 500 GC/FID and GC/MS for P3).

3. Results and discussion

We will first present results and discussion about the photodegradation carried out in the various photoreactors, then we will try to compare the phenomenon in three different conditions and in gaseous phase as well as at the photocatalyst surface.

3.1. P1: static photoreactor and study at the photocatalyst surface

Fig. 5 shows the infrared spectra of surface species adsorbed on TiO₂ during UV irradiation at 298 K. In these experiments toluene and air were both introduced in the IR cell (1 Torr of toluene with 760 Torr of air). The spectrum Fig. 5a was recorded before irradiation. The spectra Fig. 5b and c were recorded after 20 and 70 min of irradiation, respectively. During irradiation, IR bands corresponding to adsorbed toluene decrease. On the other

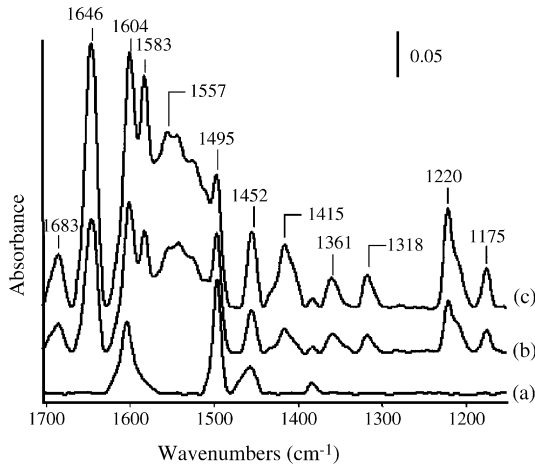


Fig. 5. Infrared spectra of toluene adsorbed on TiO_2 surface (in presence of 1 Torr of toluene and 760 Torr of air in gas phase): (a) before irradiation; (b) after 20 min of UV irradiation; (c) after 70 min of UV irradiation.

hand new IR bands with increasing intensity during irradiation were detected.

Many studies report that benzaldehyde and benzoic acid are intermediates for the partial oxidation of toluene [9,10]. To confirm their formation at the TiO_2 surface, benzaldehyde and benzoic acid were adsorbed on fresh TiO_2 .

Comparison between spectra of adsorbed benzaldehyde and benzoic acid (not shown here) on fresh TiO_2 and spectra obtained during toluene degradation confirmed the presence of benzaldehyde and benzoic acid at the TiO_2 surface.

The 1220, 1583, 1646 and 1683 cm^{-1} bands increasing during toluene degradation can be attributed to adsorbed benzaldehyde. The IR bands at 1415 cm^{-1} correspond to adsorbed benzoic acid. The IR bands at 1557 and 1360 cm^{-1} may be assigned to strongly adsorbed species such as formates.

Fig. 6 shows the integrated areas of the IR bands corresponding to the adsorbed species (benzaldehyde and benzoic acid) and the height of the IR band due to formates relative to irradiation time.

As we can see, in our experimental conditions, benzaldehyde formed at the beginning of the irradiation, accumulated at the TiO_2 surface, reached a maximum at about 250 min of irradiation. The results clearly show that benzaldehyde is the first intermediate formed during toluene oxidation; during irradiation,

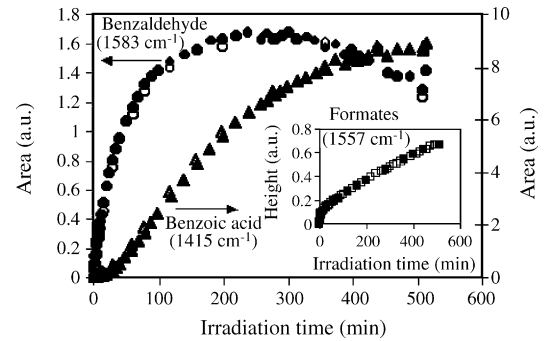


Fig. 6. Integrated area (or height) of the IR bands due to adsorbed species (benzaldehyde, benzoic acid and formates) formed during photocatalytic oxidation of toluene.

benzoic acid also accumulated at the surface, its formation is slower than that of benzaldehyde.

The insert shows that adsorbed formate species are also present and their amount increases during the photocatalytic process. These results can show a possible momentaneous deactivation of TiO_2 during the photocatalytic process.

3.2. P2: dynamic photoreactor and high toluene concentration: gaseous phase study

The kinetic of toluene photodegradation is evaluated by measuring the outlet toluene concentration. Experimental conditions are as following: $1.6 \times 10^{-5} \text{ m}^3 \text{ s}^{-1}$ inlet flow, $3.59 \times 10^{-3} \text{ g m}^{-3}$ toluene concentration in inflow. The inlet concentration is maintained constant and stable during the whole experiment. At the start of UV illumination, the outlet concentration decreases until reaching a constant value corresponding to the steady state condition of the reactor. Fig. 7a represents the variation of the concentration ratio C/C_0 , where C is the outlet toluene concentration and C_0 the inlet toluene concentration related to the experimental time.

Another study proves that the photoreactor could be assimilated to a continuous stirred flow tank reactor in which pollutants residence time is 0.2 min. Under these conditions, in steady state conditions, the toluene mass balance leads to the determination of the degradation rate r given by the following relation: $Q \times C_0 = r \times S + Q \times C$ where $[r] = \text{g m}^{-2} \text{ s}^{-1}$, Q the flow rate ($\text{m}^3 \text{ s}^{-1}$) and S is the illuminated photocatalyst media (m^2).

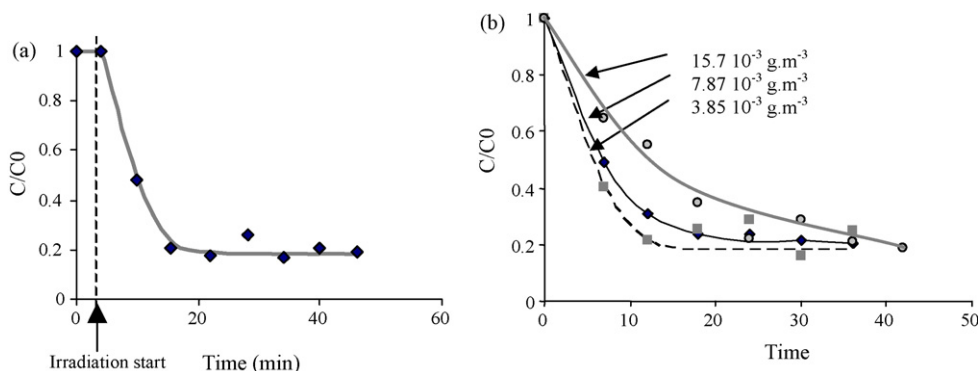


Fig. 7. (a) Toluene photocatalysis; (b) effect of toluene concentration.

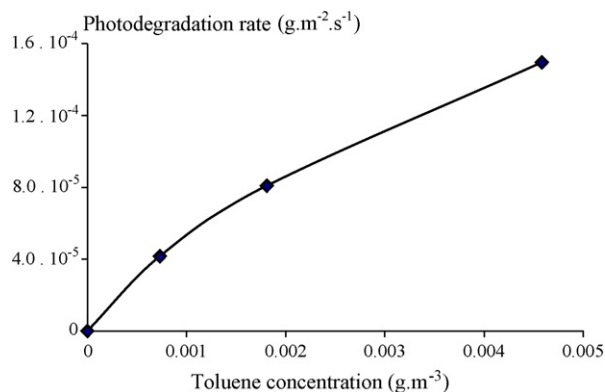


Fig. 8. Toluene degradation rate vs. toluene concentration.

The same experiments were carried out with various inlet toluene concentrations (Fig. 7b). It is observable that even at high toluene concentration the photodegradation yield is very high: conversion rates are on average 81, 77 and 71% with respectively, 3.85×10^{-3} , 7.87×10^{-3} and $15.7 \times 10^{-3} \text{ g m}^{-3}$ of toluene concentration in the inflow and with 10% of relative humidity. A lower efficiency is observed when the toluene inflow concentration increases.

Fig. 8 plots the toluene degradation rate versus toluene outlet concentration. Under the selected running conditions, the specific flow rate (Q/S) is about $1.33 \times 10^{-2} \text{ m s}^{-1}$.

From Langmuir–Hinshelwood model, which is the most acceptable for photodegradation mechanisms, the photodegradation kinetic rate has the general following expression:

$$r = k \frac{K_{\text{ads}} C}{1 + K_{\text{ads}} C + \sum_i K_{\text{des}_i} C_{\text{degradation products}}}$$

where k is the apparent photodegradation constant, K_{ads} and K_{des} are respectively the adsorption constant of toluene on TiO_2 and the desorption constant of photoproducts from TiO_2 , C and $C_{\text{degradation products}}$ represent respectively the toluene concentration in the outflow, which is the same in the photoreactor, and the photoproducts adsorbed on TiO_2 concentration. With a continuous stirred flow tank photoreactor, it is a common method to consider that photoproduct adsorption and desorption are not a competitive phenomena with toluene adsorption. These remarks lead to the determination of k and K_{ads} , without taking in account the expression $K_{\text{des}} C_{\text{degradation products}}$. This is possible by plotting the graph $1/r$ versus $1/C$. The determined parameters are: $k = 2.69 \times 10^{-4} \text{ g m}^{-2}$ and $K = 247.5 \text{ m}^3 \text{ kg}^{-1}$.

These results are similar with those observed in the literature.

3.3. P3: dynamic photoreactor and low toluene concentration

With this photoreactor, the photocatalytic degradation of toluene is evaluated by measuring the concentration at the inlet and the outlet of the reactor.

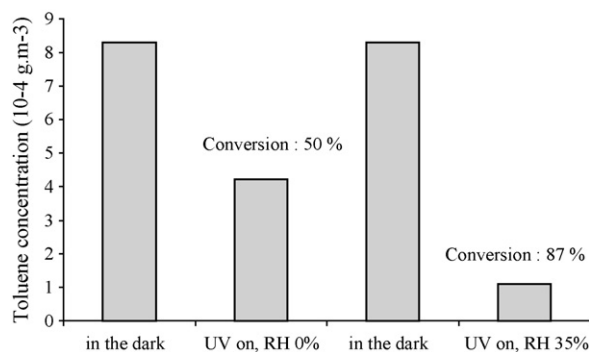


Fig. 9. Toluene conversion without water and with 35% relative humidity.

Table 1
Toluene photodegradation rate

	Photodegradation rate, r ($\text{g m}^{-2} \text{ s}^{-1}$)
RH 0%	8.0×10^{-7}
RH 35%	1.4×10^{-6}

The experiments presented in this paper are performed in the following conditions:

- initial toluene concentration: $7.8 \times 10^{-4} \text{ g m}^{-3}$;
- flow rate in the reactor: 0.15 L min^{-1} ;
- relative humidity: 0 and 35%.

Fig. 9 shows the conversion of toluene without water and with a relative humidity of 35% after 20 min of irradiation.

This result confirms that water is an important parameter for the photocatalytic degradation of VOC.

As it is done with the P2 photoreactor, the photodegradation rate can also be calculated. The results are given in Table 1.

Analysis of the gas phase at the outlet of the reactor was performed in order to identify some degradation products in the gas phase. For this purpose, the sampling volume was increased (sampling flow rate: 0.03 L min^{-1} during 20 min). No degradation products were identified in the gas phase using GC–MS analysis.

These observations are in agreement with previous results obtained with the FT-IR apparatus (P1). Using this technique, we are able to measure the activation energy of desorption of VOC on TiO_2 .

The results for toluene, benzaldehyde and benzoic acid (both are expected as degradation products) are presented in Table 2.

These values show that benzaldehyde and benzoic acid are strongly adsorbed on TiO_2 . These results confirm that these degradation products, if they are formed, are probably adsorbed on TiO_2 and not identified in the gas phase at the outlet of the

Table 2
Activation energy of desorption on PC500 TiO_2

	Activation energy of desorption (kJ mol^{-1})
Toluene	88
Benzaldehyde	123
Benzoic acid	>130

reactor. This was observed in both experiments with continuous photoreactors P2 and P3, which have different running conditions.

4. Conclusions

This research program aimed to study different mechanisms of toluene photocatalysis with different scales of running conditions (especially concentration). We use three photoreactors, one with static flow conditions to observe mechanisms at the photocatalyst/gas interface, and two others one with dynamic flow conditions and analysis of the gaseous phase. We show that one of the most important steps in the photodegradation is the VOC and photoproduct adsorption and desorption from the photocatalyst. This study highlights that it is not possible to conclude on pollutant degradation and mineralisation without taking in account the adsorbed photoproducts; their desorption and then their photodegradation depend on the relative humidity in the gaseous phase and on the activation energy of desorption.

Moreover, the PC500 TiO₂ is a very competitive photocatalyst support: at high toluene concentration, the disappearance is on average 80% compare to the size of the photoreactors applied to the gaseous depollution.

Acknowledgements

This project is funded by Rhône-Alpes Region. The authors would like to thank Groupe de Recherche sur l'environnement et la Chimie Atmosphérique) from Université Joseph Fourier Grenoble I, France, Laboratoire d'Application de la Chimie à l'Environnement (LACE), Université Claude Bernard Lyon I, France, and TERA Environnement and Ahlstrom Research and Services, both industrial firms.

References

- [1] J. Zhao, *Build. Environ.* 38 (2000) 645–654.
- [2] F.D. Yu, L.A. Luo, G. Grevillot, *J. Chem. Eng. Data* 47 (2002) 467–473.
- [3] A. Mills, *J. Photochem. Photobiol. A: Chem.* 108 (1997) 327–336.
- [4] P.A. Deveau, P.X. Thivel, F. Delpech, P. Kaluzny, *Proceedings of the 7th World Congress on Chemical Engineering*, Glasgow, July 10–14, 2005.
- [5] F. Arzac, C. Ferronato, D. Bianchi, J.-M. Chovelon, *Proceedings of the 4th International Conference on Photochemical Conversion and storage of Solar Energy*, Paris, July 4–9, 2004.
- [6] A.J. Maira, et al., *J. Catal.* 202 (2001) 413–420.
- [7] G. Martra, et al., *Catal. Today* 53 (1999) 695–702.
- [8] R. Mendez-Roman, N. Cardona-Martinez, *Catal. Today* 40 (1998) 353–365.
- [9] V. Augugliaro, et al., *Appl. Catal. B: Environ.* 20 (1999) 15–27.
- [10] M.C. Blount, J.L. Falconer, *Appl. Catal. B: Environ.* 39 (2002) 39–50.